



Low-pressure hydrothermal processing for conversion of polystyrene into oils

Clayton Gentilcore^a, Kai Jin^a, Genesis Barzallo^b, Petr Vozka^b, Nien-Hwa Linda Wang^{a,*}

^a Davidson School of Chemical Engineering, College of Engineering, Purdue University, West Lafayette, IN 47907, United States

^b Department of Chemistry and Biochemistry, College of Natural and Social Sciences, California State University, Los Angeles, CA 90032, United States

ARTICLE INFO

Keywords:

Hydrothermal processing
Low-pressure
Polystyrene
BTEX
Aromatic chemicals
Plastic co-processing

ABSTRACT

Global polystyrene (PS) waste accumulates at a rate of 28 million tons annually, while recycling rates stay at 1.3 %. PS degrades into microplastics, releasing various chemicals that affect ecosystems and human health. Conventional waste treatment methods are ineffective in reducing PS waste accumulation. This study developed batch low-pressure hydrothermal processing (LP-HTP) methods to convert PS to oils. Oil yields of 96–99 % were obtained with 1–2 % char and up to 2 % gas at average temperatures of 341–424 °C for 19–75 minutes. Reversible reactions between monomers (C₆–C₉) and poly-aromatics (C₁₀–C₂₀₊) were found to limit monomer yields. A two-step kinetic model accounting for the reversible reactions was developed. Temperature histories of the batch experiments were considered such that the estimated kinetic parameters were independent of reactor heating or cooling rates. The predicted yields of monomers and poly-aromatics agreed with experimental yields to within 6 %. The model predicted increasing monomer yields with decreasing PS loadings. This predictive model can aid future process optimization and scale-up. PS and polyolefins were co-processed to produce oils with 87 % yields and higher aromatic contents than oils produced from polyolefins alone. LP-HTP methods required no catalyst, had higher oil yields and less char formation than pyrolysis, and used much lower operating pressures and energy than supercritical water liquefaction. The methods also potentially have lower environmental impacts and 4.7 times higher energy recovery than incineration. The oils from LP-HTP, if separated into pure monomers, can be used as chemical feedstocks to achieve a circular use of hydrocarbons.

1. Introduction

1.1. Background

As of 2021, approximately 9 billion tons of plastic waste have been generated globally. Plastic waste generation rates have reached 400 million tons per year and continue to increase exponentially [1–3]. Only about 9 % of this plastic waste is recycled, and 12 % is incinerated. The remaining 79 % of plastic waste, totaling over 7 billion tons, is accumulating in landfills, surrounding ecosystems, and oceans [1,4]. These plastic wastes degrade over time into microplastics and nanoplastics,

releasing over 10,000 chemicals such as phthalates, biphenyls, and perfluorinated compounds into the environment. These toxic chemicals, acting as carcinogens, endocrine disruptors, and neurotoxins, negatively affect humans, animals, plants, and various ecosystems [3,5].

The majority (63 wt%) of plastic wastes are polyolefins, or high-density polyethylene (HDPE, Type 2, 17 wt%), low-density polyethylene (LDPE/LLDPE, Type 4, 23 wt%), and polypropylene (PP, Type 5, 23 wt%) [4,6]. Earlier studies converted polyolefins to oils with 87–91 % yields [7–9]. Polystyrene (PS, Type 6) accounts for 7 wt% of global plastic waste, or about 28 million tons produced annually [4]. PS is commonly used for single-use food packaging and containers [3]. As

Abbreviations: ADP, Abiotic Depletion Potential; AP, Acidification Potential; BTEX, Benzene-Toluene-Ethylbenzene-Xylenes; C#, Carbon Number; CFC, Chlorofluorocarbon; CHP, Combined Heat and Power; EP, Eutrophication Potential; FID, Flame Ionization Detection; GC, Gas Chromatography; GHG, Greenhouse Gas; GWP, Global Warming Potential; HDPE, High-Density Polyethylene; HP/HT, High-Pressure High-Temperature; LDPE, Low-Density Polyethylene; LLDPE, Linear Low-Density Polyethylene; LP-HTP, Low-Pressure Hydrothermal Processing; MS, Mass Spectrometry; OLD, Ozone Layer Depletion Potential; POCP, Photochemical Ozone Creation Potential; PP, Polypropylene; PS, Polystyrene; SWL, Supercritical Water Liquefaction.

* Corresponding author.

E-mail addresses: cgentilc@purdue.edu (C. Gentilcore), jin283@alumni.purdue.edu (K. Jin), gbarzal@calstatela.edu (G. Barzallo), pvozka@calstatela.edu (P. Vozka), wangn@purdue.edu (N.-H.L. Wang).

<https://doi.org/10.1016/j.jece.2024.113836>

Received 24 May 2024; Received in revised form 12 July 2024; Accepted 12 August 2024

Available online 13 August 2024

2213-3437/© 2024 Published by Elsevier Ltd.

reported in 2019, only 1.3 % of PS waste produced globally was recycled because of limitations in available PS waste treatment methods [10–12]. Microplastics and toxic chemicals released from PS waste can lead to tissue inflammation and cancer in humans [13].

1.2. Literature review on PS recycling and conversion methods

Current commercial PS treatment methods include incineration and mechanical recycling. The advantages, disadvantages, limitations, and product yields from each method are compared in detail in Table S1. Incineration combusts PS or complex plastic mixtures for energy production. Incineration for combined heat and power (CHP) recovers 41–85 % of the embodied energy content of PS (40 MJ/kg) [14–15]. However, incineration solely for electricity generation only recovers 20–35 % of the energy content [15–17]. Because of this low energy efficiency combined with electricity market prices, waste-to-energy incineration requires higher tipping fees (\$80–\$100/ton) than landfilling (\$55/ton) [18]. Furthermore, when combusting PS, high greenhouse gas (GHG) emissions and toxic compounds such as dioxins are released [6,15,17].

Mechanical recycling can be used to remelt and remold PS waste into new products. However, this process can only be done up to 10 times before the PS structure becomes too degraded, resulting in the incineration or landfilling of the weakened PS. Some PS, such as expanded polystyrene (EPS), can be difficult to collect and recycle due to their low densities, requiring “de-foaming” procedures prior to recycling. Furthermore, the unintended mixing of different types of polymers or plastics with different additives or colors can alter the mechanical properties or appearances of the plastics, making them undesirable for consumer use [6,19–20].

Lab-scale polymer dissolution methods by selective dissolution and precipitation can effectively remove dyes and additives from sorted PS waste to recover pure PS. However, some of the solvents used for polymer dissolution of sorted PS waste are toxic. Furthermore, in lab-scale studies, high volumes of solvents were required for treating complex mixtures of PS and other plastic wastes, resulting in high solvent recovery costs [21–22]. Because mechanical recycling and polymer dissolution methods have limitations, methods that produce valuable chemical feedstocks from PS wastes have the potential to encourage higher PS recycling rates.

Feedstock recycling by pyrolysis methods can convert PS waste to oils under an inert atmosphere. These oils contain valuable chemicals, including styrene and BTEX (benzene, toluene, ethylbenzene, and xylenes) monomers [23]. A detailed review of pyrolysis literature for PS conversion is included in the Supplementary Materials (Table S2). Pilot-scale (10 tons/day) continuous processes have converted PS waste to oil, but reported styrene yields were limited to 11 % [24–26]. Pyrolysis methods for PS conversion have also been studied at lab-scale (grams of feedstock). Non-catalytic pyrolysis studies reported yields of up to 69 % mono-aromatics, or “monomers,” in the carbon number range of C₆–C₉ [27–31]. These monomer yields were increased to up to 80 % using catalysts, such as NaCl with copper oxide [29] or potassium-promoted Fe–Al₂O₃ [30]. Micro-pyrolysis studies (at the microgram scale) reported yields of up to 89 % monomers, but these results have not been confirmed with larger-scale studies [32]. However, high char formation of 2–34 % in various studies limited oil yields to 92 % [25–29]. This high char formation can cause mechanical issues and catalyst deactivation, further limiting oil and monomer yields [33]. Furthermore, BTEX yields were limited to 20 % [25–29].

Lab-scale feedstock recycling methods of supercritical liquefaction converted PS to oils at temperatures of 310–550 °C in supercritical water or other solvents (Table S3) [34–36]. For water to be in the supercritical state, its temperature and pressure must be above the critical conditions of 373 °C and 22 MPa, respectively. In supercritical water liquefaction (SWL), water acts as a diluent, suppressing higher-order reactions of char formation from poly-aromatics [7–9]. Decreased char formation

resulted in increased oil yields (~99 %) [34–35]. The oil contained up to 53 % monomers, composed mostly of either BTEX or styrene [34]. While micro-SWL studies with milligrams of PS feed reported monomer yields of 74 %, these results have not been confirmed with larger-scale studies [35]. However, high water loadings in SWL (up to 95 wt% H₂O) resulted in high operating pressures (>22 MPa), requiring increased capital and operating costs if scaled up [7–9,34,37]. New feedstock recycling methods that achieve higher oil, monomer, and BTEX yields with minimal char formation and lower operating pressures, such as those developed in this study, are needed to more effectively reduce PS waste accumulation.

Promising feedstock recycling methods of low-pressure hydrothermal processing (LP-HTP) have been developed for conversion of polyolefins to oils in previous studies [9,38]. LP-HTP used lower water loadings (5 wt% H₂O) than SWL, resulting in increased productivity, lower operation pressures (2–3 MPa), and reduced capital and operating costs [9,37–38]. Despite the lower water loadings, char formation was minimal, resulting in high oil yields of 87 wt% from polyolefins [9,38]. However, no previous studies developed LP-HTP methods for PS conversion or for co-processing PS and polyolefin mixtures. This study developed LP-HTP methods for PS conversion and discusses the benefits of using LP-HTP methods over other treatment or conversion methods, such as landfilling, incineration, pyrolysis, or SWL. The oil, gas, and char yields and product recovery efficiency from LP-HTP methods developed in this study are compared with those of conventional and lab-scale methods in Table 1.

1.3. Research objective and specific goals

The overall objective of this study was to develop efficient and environmentally-friendly methods for converting PS and mixtures of PS with polyolefins to valuable oils. The specific goals of this study were the following: (1) Determine the impacts of various water loadings, reaction temperatures, and reaction times on yields of oil, monomers, and BTEX from PS. (2) Understand the depolymerization kinetics to develop a kinetic model and estimate intrinsic kinetic parameters for PS conversion. (3) Use the kinetic model to determine reaction conditions for maximizing monomer yields. (4) Test potential of co-processing PS with polyolefins. (5) Compare estimated energy recovery and environmental impacts of LP-HTP methods to those of other PS treatment methods, including landfilling, incineration, pyrolysis, and supercritical water liquefaction (SWL).

Efficient LP-HTP methods were developed to convert polystyrene to oils with 99 % yields and less char than pyrolysis (Table 1). The developed methods had lower operating pressures and required less energy than SWL. Previous pyrolysis or SWL decompositions estimated kinetic parameters for a one-step reaction of PS decomposition through free-radical chain mechanisms [28,34,39–41]. However, in this study, reversible reactions between poly-aromatics (C₁₀–C₂₀₊) and monomers (C₆–C₉) were found to limit monomer yields. Therefore, a two-step kinetic model for PS conversion to poly-aromatics and monomers in LP-HTP was developed to facilitate future process optimization and scale-up. This study found that PS and polyolefins can be co-processed into oils with 87 % yields and higher aromatic contents than the oils produced from polyolefins alone. Co-processing of the plastic mixtures would reduce the costs for sorting and separation before conversion. LP-HTP can achieve higher energy recovery and have lower environmental impacts than incineration. The efficient LP-HTP methods can convert PS or mixtures of PS with polyolefins to oils, which can be purified to produce chemical feedstocks. The methods, if upscaled for commercial production, can help develop a circular use of hydrocarbons and reduce PS waste accumulation and associated environmental pollution.

2. Experimental materials and methods

To meet the goals of this study, conversion experiments using PS

Table 1

Product yields and normalized product recoveries.

Methods and Yields	Oil [wt%]	Monomer (C ₆ -C ₉) [wt%]	BTEX [wt%]	Gas [wt%]	Char [wt%]	Product Recovery
Landfilling	N/A	N/A	N/A	N/A	N/A	0 %
Incineration [6,14–18]	N/A	N/A	N/A	N/A	N/A	35–85 %
Mechanical Recycling [6,19–20]	N/A	N/A	N/A	N/A	N/A	80–85 %
Polymer Dissolution [21–22]	N/A	N/A	N/A	N/A	N/A	80 %
Non-Catalytic Pyrolysis [27–31]	62–92 %	38–69 %	2–11 %	3–45 %	2–34 %	62–92 %
Supercritical Water Liquefaction (SWL)	96–99 %	53–59 %	46–51 %	Up to 3 %	Up to 1 %	96–99 %
[34] and SWL Results from This Study						(at 24–32 MPa)
This Study: Low-Pressure Hydrothermal Processing (LP-HTP)	96–99 %	Up to 67 %	Up to 60 %	Up to 2 %	1–2 %	96–99 %
						(at 2–3 MPa)

standard were designed and conducted at various water loadings, temperatures, and times. Six experiments at various water loadings (0, 5, 64 wt%) were done to study the impacts of water loading on oil and monomer (C₆-C₉) yields (Table S4). Fifteen experiments were conducted to find the minimum conversion temperature and to study the impacts of different reaction temperatures and times on PS conversion and product yields (Table S5). Kinetic pathways were proposed and used to build a kinetic model. Product yields and temperature histories from 14 experiments were used for kinetic parameter estimation. Nine additional experiments were then used to verify the model and the kinetic parameters (Table S6). PS and polyolefin co-processing was tested at conditions which produced high oil yields from the individual polymers (Table S7). Oil, gas, and solid yields were measured after each experiment. Oil compositions consisting of monomers (C₆-C₉), dimers (C₁₀-C₁₇), and heavy aromatics (trimers and heavier poly-aromatic hydrocarbons, C₁₆-C₂₀₊) were analyzed by batch distillation and by GC-MS/FID and GC×GC-FID methods.

2.1. Feedstocks used in experiments

Three polymer standard feedstocks were converted in this study. The first feedstock was standard polystyrene (PS) pellets with a characteristic diameter of 2–4 mm and weight-average molecular weight (M_w) of 192,000 g/mol, acquired from Sigma-Aldrich (St. Louis, MO). This feedstock was selected to study the intrinsic kinetics of pure PS conversion without the presence of any additives or fillers. Furthermore, to study the co-processing of PS with polyolefins, standard polyolefin feedstocks of HDPE (M_w of 180,000 g/mol) and PP (M_w of 250,000 g/mol), both acquired from Sigma-Aldrich and having 2–4 mm characteristic diameters, were used. These polyolefin feedstocks were extensively utilized in previous SWL and LP-HTP studies [7–9].

2.2. Equipment and procedure for plastic conversion

A 500-mL Series 4575A HP/HT (high-pressure high-temperature) batch Parr reactor from the Parr Instrument Company (Moline, IL) was used for all conversion experiments. All but two experiments were conducted with 40 g of plastic feedstock, equivalent to a polymer loading of 80 g/L. The internal stirrer of the batch reactor provided sufficient mixing when using 40 grams of feedstock. If more feedstock was used, the heating rate of the reactor would be slower. Two experiments used 20 g (40 g/L loading) to study the impacts of lower PS loading on oil and monomer (C₆-C₉) yields.

Various water loadings were tested, including 0 g H₂O (0 wt%) for conversion under an inert atmosphere with no water, 2 g H₂O (5 wt%) for LP-HTP, and 70 g H₂O (64 wt%) for SWL. These three water loadings were chosen based on extensive previous studies with polyolefins [7–9, 38]. Previously, water loadings of 0, 5, 15, 32, and 64 wt% were tested for polyolefin conversion. No significant differences in oil, gas, and solid yields were observed when using 5, 15, or 32 wt% water loadings [9]. Since 5 wt% water loading required the least amount of water and had the lowest operating pressure in the 5–32 wt% range, 5 wt% water

loading was preferred and was found to be the best water loading in the previous polyolefin studies. For these reasons, water loadings of 0, 5, and 64 wt% were tested in this study, resulting in water pressures of up to 1.5 MPa for 5 wt% water loading and up to 33 MPa for 64 wt% water loading. The water used in experiments was first purified by a Milli-Q water purification system and then degassed for 30 minutes prior to use [7–9]. Prior to conducting experiments, the feedstock and any required water were added to the reactor, and the reactor was sealed. The heating jacket was then raised up to the reactor, and the reactor top was insulated with fiberglass and aluminum sheets to reduce heat loss. The reactor was then purged three times with 1 MPa-gauge N₂ to remove any air and prevent combustion. Finally, before turning on the heating jacket, the magnetic drive motor of the reactor was started to provide stirring at a constant rate of 100 RPM for all experiments.

During each experiment, the reactor and its contents were heated using the heating jacket to the desired set temperature (T_S). This T_S was then maintained for the desired set time (t_S). After the t_S had elapsed, the reactor and its contents were cooled. Most experiments used compressed air flowing through the internal cooling loop of the reactor to provide cooling. Experiments were also conducted with faster cooling methods, such as chilled water and ice water, at the same T_S and t_S to test if different cooling rates had any significant effect on PS conversion.

Because of slow heating and cooling rates specific to the Parr reactor used, as shown in Fig. S1, the desired T_S could not be reached instantaneously. As a result, conversion occurred before the T_S was reached and after the t_S had elapsed. The full temperature histories were considered in building the kinetic model and estimating the intrinsic parameters for predicting PS conversion. Accounting for the detailed temperature histories ensured that the estimated kinetic parameters were independent of the heating and cooling histories of the specific equipment used. As a result, these parameters can also be used in future studies for developing continuous processes with fixed operating temperatures.

Variables of a fixed average temperature and total reaction time can help future process operation at different scales or in continuous modes. In this study, to simplify the description of detailed temperature histories, variables of effective average reaction temperature (T_A) and effective reaction time (t_E) were developed [38]. No PS conversion was observed at or below 300°C in this study. This observation agreed with previous studies that conducted thermogravimetric analysis of PS, in which minimal PS conversion was observed below 300°C [28,39]. Therefore, with no conversion occurring below 300°C, the effective reaction time (t_E) was defined as the time above 300°C in the temperature history of each experiment. The effective average reaction temperature (T_A), defined as the average temperature at which conversion occurred, was calculated from the area under the temperature history curve above 300°C divided by t_E (Fig. S2). The values of T_A and t_E differ from the respective values of T_S and t_S because of the slow heating and cooling rates of the available Parr reactor used. The values of T_A and t_E for each experiment are compared with their respective values of T_S and t_S in Tables S4–S7.

2.3. Experimental designs

Preliminary LP-HTP experiments showed that using a set temperature (T_S) of 490°C for PS conversion resulted in high oil and monomer yields. This T_S of 490°C was then used for conversion at different water loadings and set times (t_S). Experiments using a lower T_S of 450°C and longer t_S were also conducted. The experiments at 450°C were designed and performed to have average reaction temperatures (T_A) similar to those of experiments at 490°C (Table S4). Experiments with different water loadings were conducted to compare the impact of varying water loading on operation pressure and yields of oil, monomers, gas, and char from PS conversion.

In total, 24 experiments of PS conversion were conducted. Fifteen experiments for converting PS standard with 80 g/L PS loadings and 5 wt% water loadings were conducted at various reaction temperatures and times, with results shown in order of increasing values of T_S and t_S . These 15 experiments were done to study the impacts of varying reaction temperature and time on oil and monomer yields. Experiments 1–2 focused on operating at T_S of 300–350°C for t_S of 30 minutes to estimate the minimum temperature for PS conversion. PS conversion was then conducted at increasing T_S of 400–490°C for t_S of 10 minutes to study the impact of varying T_S on oil and monomer yields until increased char formation was observed in Experiment 14. Then, PS conversion at T_S for 490°C for t_S of 0–15 minutes (Exp. 11–15) was conducted to study the impact of varying t_S on oil and monomer yields until increased char formation was observed in Experiment 15 using a t_S of 15 minutes. Finally, lower T_S of 425–450°C with longer t_S of 30–60 minutes were tested (Exp. 6–7, 9) to study PS conversion at T_A values (Table S5) similar to Experiments 11–15. These experiments were used to estimate intrinsic kinetic parameters to describe PS conversion, with Experiment 15 excluded because of high char formation observed.

Different cooling methods with increasing cooling rates were used to study the impact of varying cooling rates on oil and monomer yields. These cooling methods included compressed air, chilled water, and ice water. Using different cooling methods in these experiments allowed variations in cooling rates to be accounted for when determining and verifying the intrinsic kinetic parameters. Yield results obtained with various cooling rates (Exp. 11–12) were included in the 14 experiments used for estimating intrinsic kinetic parameters (Table S5). Yield results with different cooling rates (Exp. 16–17) were also included in the subsequent experiments for kinetic model verification (Table S6).

Nine additional experiments were conducted to verify the predictive nature of the kinetic model and the model parameters. Two experiments (Exp. 5B, 13B) conducted were replicates of earlier experiments (Exp. 5A, 13A) to confirm experimental reproducibility. As the kinetic model predicted higher monomer yields with increasing temperature and time, three experiments were conducted at higher T_S for shorter t_S (Exp. 16–18) compared to Experiments 11–15. Similarly, two experiments were conducted at lower T_S for longer t_S (Exp. 19–20) to study PS conversion at T_A values similar to Experiments 14–15 and 18 (Tables S5–S6). Finally, two experiments were conducted with lower PS loadings of 40 g/L (Exp. 21–22) at values of T_S and t_S similar to earlier experiments (Exp. 11–12, 16–17) to study the impact of lower PS concentration on oil and monomer yields (Table S6).

In this study, PS was converted to 97 % oil yields at conditions of T_A of 424°C and t_E of 75 minutes. The results of the previous study with polyolefins had 87 % oil yields at T_A of 424°C and t_E of 75 minutes [9]. Therefore, these overlapping conditions were used in the co-processing experiments with PS and polyolefins (Experiment 19-PE+PP+PS, Table S7). Co-processing experiments were conducted to study if PS and polyolefin conversion occurred independently, and to determine if co-processing increased the aromatic contents of oils compared to those from polyolefins alone.

2.4. Product collection and yield estimation procedures

The mass balance of the gas, solid, and oil produced from the PS is summarized in Eq. 1. The percentage yields of each product are calculated using Eqs. 2a–2c. After cooling the reactor to room temperature, a 0.1 MPa-gauge pressure gauge was attached to the batch Parr reactor by a threaded valve. Prior to opening the reactor, the specified valve was opened, and the internal reactor pressure was measured and recorded. If the measured pressure was above 0.1 MPa-gauge, a 0.7 MPa-gauge pressure gauge was used. The gas yield was calculated directly from this recorded pressure by the ideal gas law and based on the initial feedstock mass used (Eq. 2a). While the gas products were not analyzed in detail due to low yields, the gas compositions were estimated to have an average molecular weight similar to that of propane (C_3H_8) [9,28]. This assumed molecular weight, the 500 mL reactor volume, the ambient temperature of 20°C, and the initial feedstock mass were used to approximate the yield of gas produced (Eq. 2a).

$$m_{PS_i} = m_{PS_{Remaining}} + m_{Gas} + m_{Solid} + m_{Oil} \quad (1)$$

$$Gas\ Yield\% = \left[\frac{m_{Gas}}{m_{PS_i}} \right] \times 100\% = \left[\frac{MW_{C_3H_8} \cdot \left(\frac{P_{Gas} \cdot V_{Reactor}}{R \cdot T_{Ambient}} \right)}{m_{PS_i}} \right] \times 100\% \quad (2a)$$

$$Solid\ Yield\% = \left[\frac{m_{Solid}}{m_{PS_i}} \right] \times 100\% \quad (2b)$$

$$Oil\ Yield\% = \left[\frac{m_{Oil}}{m_{PS_i}} \right] \times 100\% = [m_{PS_i} - m_{Gas} - m_{Solid}] \times 100\% \quad (2c)$$

The solids were then separated from the liquid by removing the liquid oil and water from the reactor, leaving the solids and trace oils behind. Following this separation, the solids were collected using pre-weighed laboratory napkins or a pre-weighed glass dish. These solids were dried for 24 hours in a 70°C oven, and then weighed to measure the solid yield (Eq. 2b), with the mass of evaporated oils assumed to be polyaromatics (C_{10} – C_{20}). While not all the oil absorbed by the solid may have evaporated during the drying step, it is assumed that any remaining oil is negligible as the char yields are small (1–2 %) in most experiments conducted. Following these measurements, the oil yield was calculated by difference (Eq. 2c) based on the initial feedstock mass, the mass of any remaining feedstock, and the measured gas and solid masses produced [7–9,38]. Except for Experiment 1, where no conversion occurred and a hard PS melt was collected, all other experiments conducted achieved total conversion of PS to oil, gas, and char. To complete the mass balance if total conversion should ever not occur, a term was added to describe any remaining PS.

2.5. Batch distillation equipment and procedure for separation of oil product into fractions

Following determination of the gas, solid, and oil yields, the collected liquid product was treated with magnesium sulfate ($MgSO_4$) to absorb any water present. Specifically following experiments using 64 wt% water loadings, the oil was first separated from water using a gravity separation funnel prior to treatment by $MgSO_4$. After saving 2 g of the oil produced in each experiment for later chemical analysis, the remaining treated oil was transferred to a 250 mL round bottom flask that was then placed into a batch distillation apparatus. After insulating the round bottom flask with aluminum sheets and ensuring that cooling was provided using chilled water and a recirculating chiller, batch distillation was conducted at temperatures of up to 300°C.

Distillation was used to separate each oil sample into three fractions with adjacent boiling point ranges. The reported yields of the oil fractions were based on the weight fractions from distillation. Fraction 1

($T_{\text{Distillation}} \leq 170^\circ\text{C}$) was mostly composed of “monomers” ($\text{C}_6\text{--C}_9$), or one-ring aromatic hydrocarbons. Fraction 2 ($170^\circ\text{C} < T_{\text{Distillation}} \leq 300^\circ\text{C}$) was mostly composed of “dimers” ($\text{C}_{10}\text{--C}_{17}$), or two-ring aromatics. Fraction 3 ($T_{\text{Distillation}} > 300^\circ\text{C}$) was mostly composed of “heavy aromatics” ($\text{C}_{16}\text{--C}_{20+}$). These heavy aromatics included “trimers” ($\text{C}_{16}\text{--C}_{19}$), or three-ring aromatics, and heavier poly-aromatic hydrocarbons (C_{20+}) [42]. Fractions 2 and 3 together were described as “poly-aromatics” ($\text{C}_{10}\text{--C}_{20+}$). When conducting separation of oils from co-processing PS with polyolefins, the three respective fractions were mostly composed of “naphtha” ($\text{C}_5\text{--C}_9$), “middle distillate” ($\text{C}_{10}\text{--C}_{15}$), and “heavy oil” ($\text{C}_{16}\text{--C}_{20+}$), respectively.

2.6. Chemical analysis of oils by GC-MS/FID and GC×GC-FID

The composition of each oil sample before distillation was determined by GC-MS/FID, with detailed methods described in Table S8. While the $\text{C}_6\text{--C}_{19}$ hydrocarbons present in the oil were analyzed by GC-MS/FID, the C_{20+} hydrocarbons were too heavy to be analyzed by the GC-MS/FID method. Therefore, any remaining unknown hydrocarbons in the “heavy aromatic” fraction by weight were assumed to be C_{20+} . For oils produced from co-processed PS with polyolefins, the collected “naphtha” and “middle distillate” fractions were analyzed by GC×GC-FID, with detailed methods [9,43–44] described in Table S8.

3. Experimental results for water loading and PS kinetic model parameter estimation

Six experiments were conducted at various water loadings (0, 5, 64 wt%) to study the effects of water loading on oil, monomer ($\text{C}_6\text{--C}_9$), gas, and char yields from PS (Section 3.1). Fifteen experiments were conducted at various average reaction temperatures (T_A , $304\text{--}428^\circ\text{C}$) and effective reaction times (t_E , 19–86 min) with 80 g/L PS loadings and 5 wt% water loadings (Section 3.2). The compositions and stability of these oils were also studied over 12 months (Section 3.3). The full temperature histories and oil compositions of 14 of these experiments were used in parameter estimation for a kinetic model, as shown in Section 4.

3.1. Effect of water loading on oil yields and compositions

Experiments for converting PS standard were conducted with 0, 5, and 64 wt% water loadings. The operating conditions and yields of oil,

gas, and char from these experiments are shown in Fig. 1. Values of average temperature (T_A) and effective reaction time (t_E) of the six experiments are shown in Table S4. Detailed temperature and pressure histories of the six experiments can be seen in Fig. S3. The compositions of produced gases were not analyzed in this study because of their low yields (1–2 %).

Experiments W1–W3 were conducted at lower temperatures and longer times than W4–W6. Because of the lower temperatures, Experiments W1–W3 had higher oil yields and lower gas and char yields than W4–W6 (Fig. 1). At elevated temperatures, W5 (5 wt% water) showed reduced char formation compared to W4 (0 wt% water) because water acted as a diluent to suppress char formation [7–9]. For a similar reason, Experiments W2 and W5 (5 wt% water) also showed lower char yields (1–2 %) than those reported for pyrolysis methods (2–34 %) [27–31].

W6 (64 wt% water) had a higher gas yield than W5 (5 wt% water) because of longer effective reaction times (t_E) caused by the higher water loading (Table S4). Both experiments using 5 wt% water had higher monomer and BTEX yields (Fig. 1) than those using 0 and 64 wt% water when operating at the same set temperature (T_S) and set time (t_S). Experiments using 5 wt% water also had significantly lower operating pressures (2–3 MPa) than those of experiments using 64 wt% water (24–29 MPa, Fig. S3). A 5 wt% water loading was therefore used for the 15 subsequent experiments conducted at various temperatures and times.

3.2. Impacts of temperature and time on oil yields and compositions

Fifteen LP-HTP experiments (Experiments 1–15) were conducted to study the impacts of reaction temperature and time on oil and monomer yields. Experiment 1 showed no conversion at T_A of 304°C and t_E of 31 minutes (Table S5). With increasing reaction temperature and time in Experiments 2–15, oil yields decreased as gas yields increased (Fig. 2). At T_A exceeding 420°C (Exp. 14–15), oil yields decreased as char yields increased. Experiments 11 and 12 both used the same T_S and t_S , but employed different cooling methods to see if oil and monomer yields were affected by different cooling rates. The results showed that cooling to 300°C with compressed air over 12 minutes (Exp. 11) or cooling to 300°C with ice water over 1 minute (Exp. 12) did not significantly impact oil and monomer yields.

Monomer ($\text{C}_6\text{--C}_9$) and BTEX yields increased with increasing temperature and time, and then plateaued at monomer yields of 56–67 %

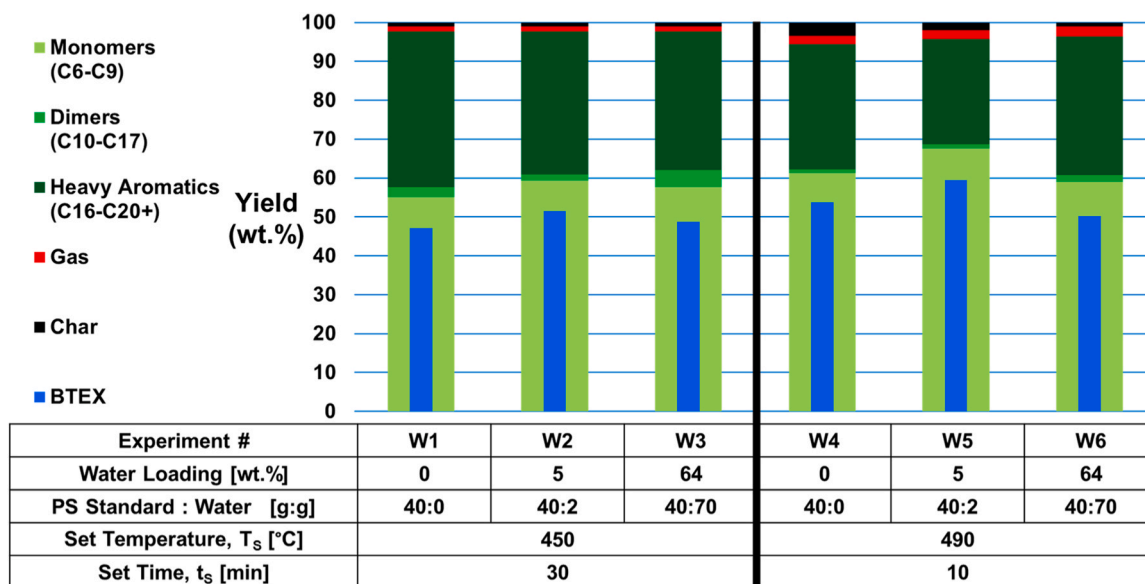


Fig. 1. Yields of monomers, BTEX, dimers, heavy aromatics, gas, and char from PS conversion experiments using various water loadings. Yield percentages are based on the PS feedstock used in each experiment.

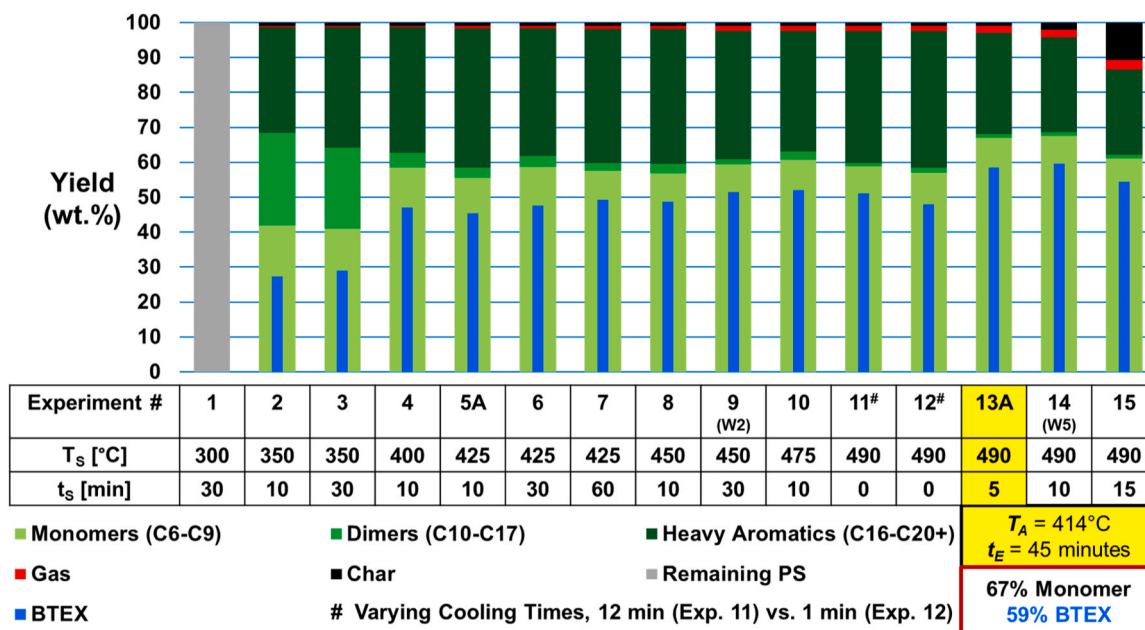


Fig. 2. Yields of monomers, BTEX, dimers, heavy aromatics, gas, and char from Experiments 1–15 for converting PS with 5 wt% water loadings at various set temperatures (T_s) and times (t_s). The numbering of the experiments was based on increasing T_s , and increasing t_s at the same T_s .

(Fig. 2). The plateauing monomer yields were observed in Experiments 4–15, with average temperatures (T_A) of 376–428°C and effective reaction times (t_E) of 31–86 minutes (Table S5). These plateauing monomer yields are plotted with their respective T_A values in Fig. S4 to better visualize this trend.

Experiment 13A resulted in the highest monomer yield of 67 %, with high oil yields (97 %) and minimal char (1 %) and gas (2 %). The dimer (C_{10} – C_{17}) yields decreased with increasing temperature and time and then plateaued at 1–4 % while heavy aromatic (C_{16} – C_{20+}) yields also plateaued at 27–40 % for Experiments 2–14 (Fig. 2). The plateauing

yields of monomers (C_6 – C_9) and poly-aromatics (C_{10} – C_{20+}) can be explained by reversible reactions between the two hydrocarbon groups. Kinetic models were built based on Experiments 1–14 to explain these plateauing yields, as discussed in Section 4. Experiment 15 was not used for kinetic parameter estimation due to high char formation (~10 %) at the high T_A of 428°C and long t_E of 55 minutes.

Detailed oil compositions for 6 experiments (Exp. 2, 4, 5A, 8, 10, 13A) with increasing values of T_A and t_E are shown in Fig. 3 and Table S9. The results show that, as PS depolymerizes into poly-aromatics (C_{10} – C_{20+}) and monomers (C_6 – C_9), their yields plateaued at 30 % and

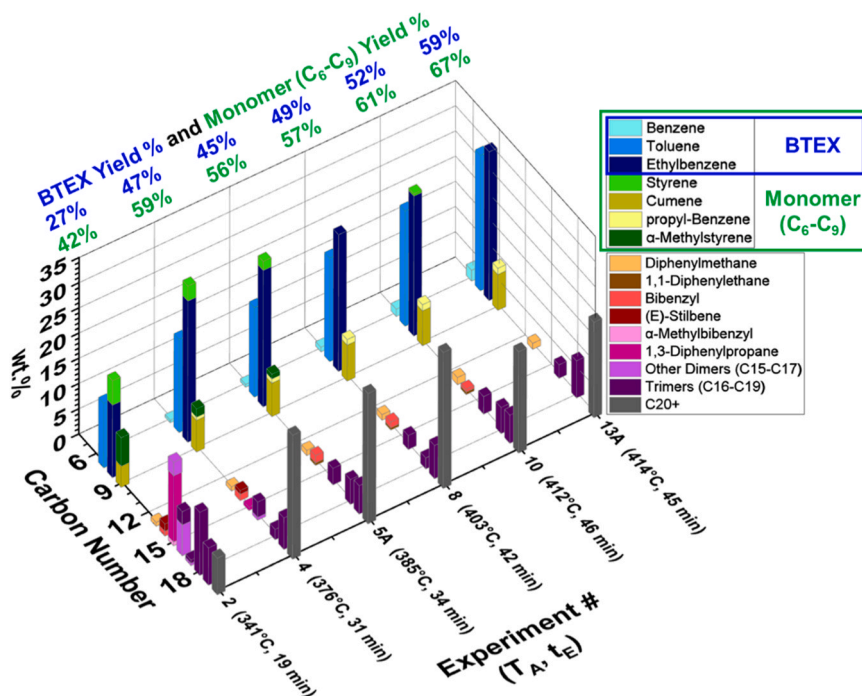


Fig. 3. Detailed oil compositions from PS conversion. Monomer (C_6 – C_9) and BTEX yields increased with increasing average temperature (T_A) and effective reaction time (t_E).

67 %, respectively. The plateaus can be explained by reversible reactions between poly-aromatics and monomers. Detailed conversion mechanisms consistent with these analytical results were developed and proposed in Eq. S1-S26. The mechanisms are consistent with previous literature studies on PS thermal decomposition [45–48] and benzyl radical combination into poly-aromatic hydrocarbons [49].

Trends of dimers (C_{10} - C_{17}) and trimers (C_{16} - C_{19}) converting to monomers (C_6 - C_9) and heavier poly-aromatics (C_{20+}) are shown between Experiments 2 and 4 (Fig. 3). Specifically, some of the dimers (orange, red, pink) and trimers (purple) in Experiment 2 converted to monomers (blue, green, yellow) in Experiment 4, as described in Eq. S1-S10. However, some of these monomers also recombine into dimers and trimers, as shown in Eq. S11-S16, and further combine to form heavier poly-aromatics (gray, C_{20+}).

Trends of specific monomers and poly-aromatics converting to other monomers are shown in results from Experiments 4–13A (Fig. 3). Styrene (light green, C_8) converted to benzene (light blue, C_6), toluene (blue, C_7), and ethylbenzene (dark blue, C_8). Similarly, α -methylstyrene (dark green, C_9) converted into cumene (dark yellow, C_9) or BTEX (blues, C_6 - C_8). Trace amounts of C_7 - C_9 monomers converted to benzene (light blue, C_6) and light hydrocarbon gases (C_1 - C_5) not present in the oils (Eq. S17-S26). Additionally, (*E*)-stilbene (dark red, C_{14}) converted to bibenzyl (light red, C_{14}), which then converted into BTEX (blues, C_6 - C_8). Furthermore, α -methylbibenzyl (light pink, C_{15}) and 1,3-diphenylpropane (dark pink, C_{15}) converted to compounds such as propyl-benzene (light yellow, C_9) or BTEX (blues, C_6 - C_8). These analytical results of monomer (C_6 - C_9) and poly-aromatic (C_{10} - C_{20+}) yields at different reaction temperatures and times were the basis for the proposed kinetic pathways shown in Fig. 4 (Section 4).

3.3. Study on oxidative stability of oils

Oils from Experiments 2–4, 5A, and 13A (Fig. 2) were stored at room temperature within glass vials in a dark, enclosed space for 12 months and then reanalyzed to study the oxidative stability of these oils. Compositions of the aged oils compared to their initial compositions are shown in Fig. S5. The differences in monomer and poly-aromatic yields observed over time for each oil sample were 2–4 %, which were within the statistical error of the GC/MS-FID method used. This reanalysis determined that no oxidized hydrocarbons were present in the aged oils, showing the oxidative stability of the oils produced from PS conversion by LP-HTP methods.

4. Kinetic modeling and intrinsic kinetic parameter estimation

The purpose of constructing a kinetic model in this study was to aid process optimization for achieving high monomer yields from PS conversion. Based on the reversible reaction behavior observed in PS conversion (Section 3), pathways and kinetic equations for a reversible kinetic model were proposed (Section 4.1). Full temperature histories and product yields from 14 batch experiments were considered in estimating the intrinsic kinetic parameters of the model (Section 4.2). As these parameters are both temperature- and equipment-independent, they can aid process scale-up in future studies.

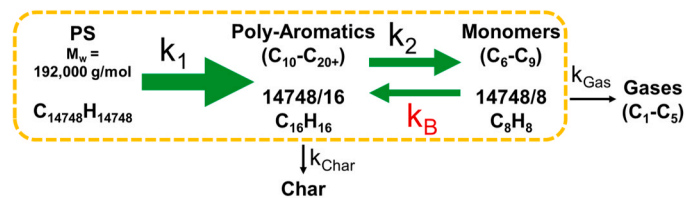


Fig. 4. Reversible kinetic model pathways for PS conversion. The slower reactions for gas and char formation (using smaller arrows) were not included in the kinetic model, as observed gas and char yields were minimal (1–2 %).

4.1. Pathways and equations of reversible kinetic model

Observed equilibrium between monomer (C_6 - C_9) and poly-aromatic (C_{10} - C_{20+}) yields (Figs. 2–3) suggested that reversible reactions occurred between these two hydrocarbon groups. To simplify kinetic model construction, similar chemical species were lumped together into “monomers” (C_6 - C_9) and “poly-aromatics” (C_{10} - C_{20+}), with average molecular weights assigned to each lumped species. As dimers (C_{10} - C_{17}) were almost completely converted in Experiments 4–14 at T_A above 375°C (Table S5, Fig. S4), the dimers were categorically combined with heavy aromatics (trimers and heavier poly-aromatics, C_{16} - C_{20+}) as “poly-aromatics”. The constructed reversible model (Fig. 4) features first-order decomposition reactions and second-order recombination reactions. The decomposition reactions include the conversion of PS to poly-aromatics (k_1) and the conversion of poly-aromatics to monomers (k_2). To simulate the reversible reactions observed, the reversible model also includes the recombination of monomers into poly-aromatics (k_B).

The reversible model (Fig. 4) consists of a mass balance equation (Eq. 3) and kinetic equations based on the concentrations of PS, poly-aromatics, and monomers. The total mass balance is based on the oil and any remaining PS. Minimal char (1–2 %) and gas (up to 2 %) yields are not considered in the kinetic model. Each kinetic rate constant is assumed to follow the Arrhenius Equation (Eq. 4). The reversible model equations (Eqs. 5–7) are assumed to follow first-order decomposition reactions (k_1 , k_2) and second-order recombination reactions (k_B).

Mass Balance and Kinetic Equations:

$$C_{PS_i} = C_{PS_f} + \frac{16}{14748} C_{PolyAro_f} + \frac{8}{14748} C_{Mono_f} \quad (3)$$

$$k_x = k_{0,x} \cdot e^{\frac{E_{a,x}}{RT_f}} \quad (4)$$

Equations for Kinetic Model with Reversible Reactions:

$$\frac{dC_{PS}}{dt} = r_{PS} = -k_1 C_{PS} \quad (5)$$

$$\begin{aligned} \frac{dC_{PolyAro}}{dt} &= -\left(\frac{14748}{16}\right) r_{PS} + r_{PolyAro} - \left(\frac{8}{16}\right) r_{Mono} \\ &= \frac{14748}{16} k_1 C_{PS} - k_2 C_{PolyAro} + \frac{8}{16} k_B C_{Mono}^2 \end{aligned} \quad (6)$$

$$\frac{dC_{Mono}}{dt} = -\left(\frac{16}{8}\right) r_{PolyAro} + r_{Mono} = \frac{16}{8} k_2 C_{PolyAro} - k_B C_{Mono}^2 \quad (7)$$

4.2. Estimation of parameters and standard errors for reversible kinetic model

The full temperature histories (Fig. S1) and the initial and final concentrations of lumped species from Experiments 1–14 (Fig. 2) were used to estimate intrinsic kinetic parameters for the reversible model (Fig. 4, Table 2). The MATLAB programs of LSQNONLIN (Non-Linear Least-Squares Fitting) and ODE45 were used to estimate best-fitting parameters by minimizing standard errors between model-predicted

Table 2

Best-fitting kinetic parameters and standard errors of reversible model.

Parameter	Values for Reversible Model
$k_{0,1}$ [min^{-1}]	6.5×10^{22}
$E_{a,1}$ [kJ/mol]	279.1
$k_{0,2}$ [min^{-1}]	69.3
$E_{a,2}$ [kJ/mol]	40.5
$k_{0,B}$ [$\text{L} \cdot \text{mol}^{-1} \cdot \text{min}^{-1}$]	95.7
$E_{a,B}$ [kJ/mol]	41.0
Standard Error for PS Yields	3.1 %
Standard Error for Poly-Aromatic Yields	6.0 %
Standard Error for Monomer Yields	5.7 %

yields and experimental results (Eq. S30-S33). The detailed procedures of parameter estimation and statistical analysis of standard errors are explained in Supplementary Section S4.

The average temperatures (T_A), effective reaction times (t_E), and normalized product yields of Experiments 1–14 (Fig. 2, Table S5) were used to estimate initial guesses for the parameters of k_0 and E_a within k_1 and k_2 (Fig. S6, Table S10, Eq. S27-S29). The initial guesses for the parameters of k_0 and E_a within k_B were based on those used for parameters within k_2 (Table S11). These initial guesses were used to obtain the best-fitting parameters and standard errors of yields for the reversible model (Fig. 4, Table 2). The parameters estimated for k_1 , describing PS depolymerization to poly-aromatics, were similar to those estimated for PS decomposition by thermogravimetric analysis in previous literature [28,39–41].

The predicted yields showed close agreement with observed product yields, with standard errors of 5.7 % for monomers and 6.0 % for poly-aromatics (Table 2, Fig. S7). These close agreements between predicted and observed results show that the reversible model can be used for predicting product yields of poly-aromatics and monomers from PS conversion to within ~6 %. The model and the kinetic parameters were then further verified with additional experiments (Experiments 5B, 13B,

16–22), as discussed in Section 5.

5. Verification and application of the kinetic model

Nine additional experiments were conducted to test reproducibility of experimental results and verify the predictions of the kinetic model at different conditions (Section 5.1). Simulations were also conducted to further investigate the impact of PS loading on yields and productivities of monomers and poly-aromatics (Section 5.2).

5.1. Comparison of experimental yields with kinetic model predictions

Observed and predicted monomer and poly-aromatic yields from the 9 experiments for kinetic parameter verification (Fig. 5(a)) agreed to within 6 % when considering the full temperature histories (Fig. 5(b)). When using T_A and t_E values of the 9 experiments (Table S6) to predict yields of monomers and poly-aromatics, similar agreements were again observed (Fig. 5(c)). The agreement between predicted and observed yields suggests that only average reaction temperatures and effective reaction times are needed to predict yields from PS conversion. This result further suggests that the kinetic model (Fig. 4) and its intrinsic

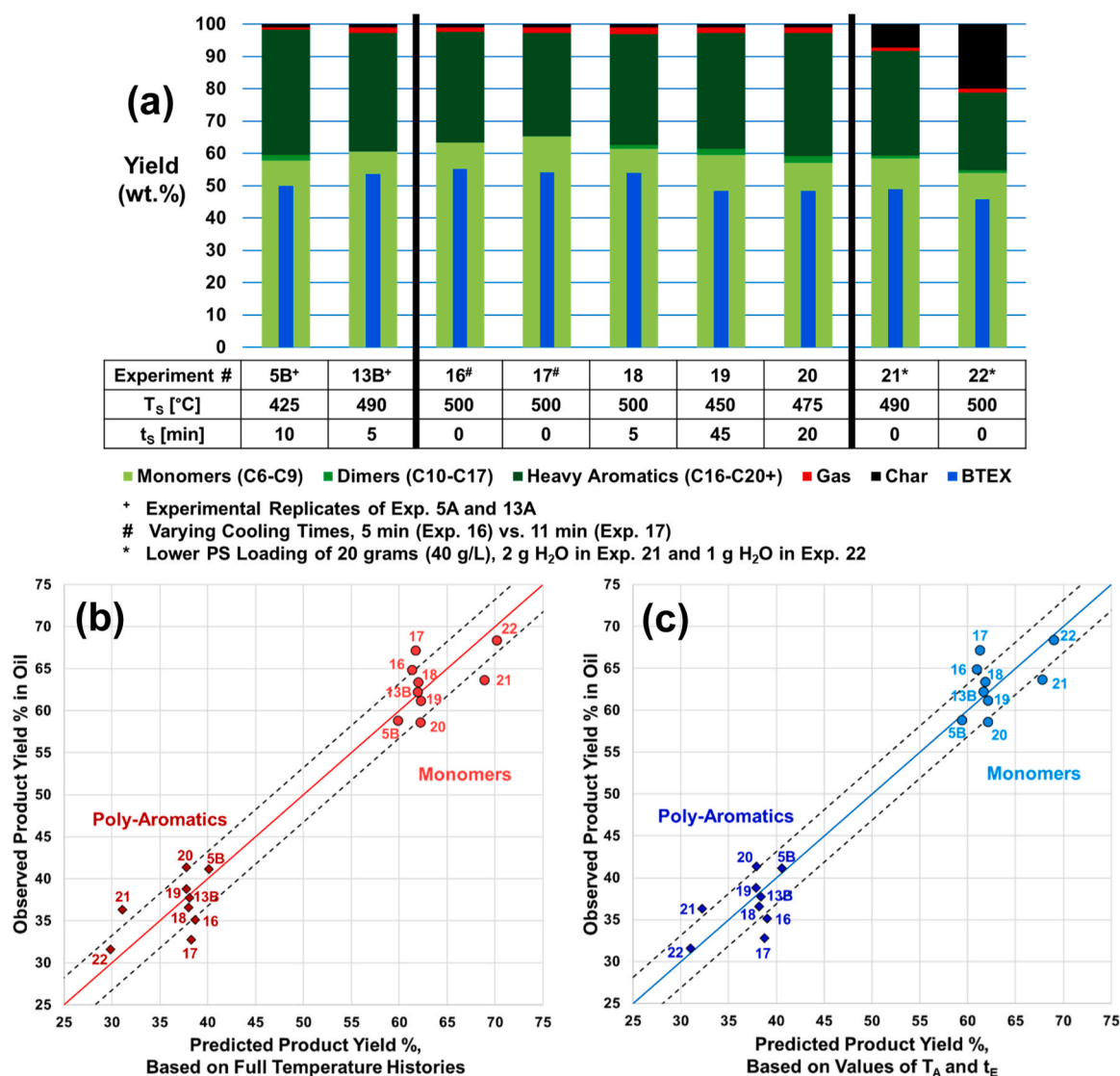


Fig. 5. (a) Yields of monomers, BTEX, dimers, heavy aromatics, gas, and char from Experiments 5B, 13B, and 16–22. Observed monomer and poly-aromatic yields were compared to model predictions based on (b) full temperature histories and (c) values of T_A and t_E of each experiment. With a t-value score of 2.896, 98 % confidence intervals for Fig. 5(b-c) are shown.

parameters (Table 2) are independent of temperature histories in the specific equipment used. This predictive kinetic model has the potential to aid future process optimization and scale-up.

Experimental replicates (Exp. 5B, 13B) had oil and monomer yields that agreed closely with those of respective previous experiments (Exp. 5A, 13A). Specifically, yields of oil, gas, and char agreed to within 1 %, and monomer and poly-aromatic yields agreed to within 6 % (Figs. 2, 5(a), Table S9). The agreements between replicated experiments support the reproducibility of these results.

Model predictions suggested that lower PS loadings will result in higher monomer yields. Experiments 21–22 were conducted to study the impacts of lower PS loading (40 g/L) on oil and monomer yields. Even at 40 g/L PS loading, where the level of PS in the reactor was below the bottom of the internal stirrer and poor mixing caused increased char formation, monomer yields of 64–68 wt% in the oil were still observed (Fig. 5(a)), agreeing with model predictions of 68–70 wt% (Fig. 5(b-c)). The impact of different PS loadings on potential monomer yields was further studied with model simulations, as shown in Section 5.2.

5.2. Modeling impact of PS loading on monomer yield and productivity

Kinetic model predictions suggest that decreasing PS loadings will result in higher monomer yields if sufficient mixing is achieved. Simulated yields of monomers and poly-aromatics from PS loadings of 4, 8, 20, 40, 80, 160, and 200 g/L are shown in Fig. 6(a). Simulations used T_A of 414°C and t_E of 45 minutes based on Experiment 13A (Table S5), which had a monomer yield of 67 % at 80 g/L PS loading (Fig. 2). Predicted monomer yields increased with decreasing PS loading, reaching as high as 90 % monomers with a PS loading of 4 g/L. However, this relatively low loading (compared to those of 40–80 g/L) could not be tested with the equipment used in this study.

The impact of different PS loadings on the reactor productivity, which is defined as the grams of products per liter of reactor, was also an important consideration. Increasing PS loadings were predicted to have higher productivities of monomers and poly-aromatics (Fig. 6(b)). While 4 g/L PS loading was predicted to result in 90 % monomers within the oil, the productivity would only be 3.6 g/L for monomers. Therefore, for future process optimization, a trade-off between monomer yield and productivity should be considered when choosing what PS loading to use.

6. Co-processing PS with polyolefins

Co-processing experiments of PS with polyolefin standards used ratios of 4.5:4.5:1 HDPE:PP:PS (Table S7), which are similar to the ratios of polyolefins and PS in global plastic wastes (63 % polyolefins, 7 % PS). Experiments using only PS (Experiment 19-PS) and only 1:1 HDPE:PP (Experiment 19-PE+PP) were also conducted to determine if the three

polymers convert independently during co-processing. Experiment 19 from Fig. 5(a) was relabeled as 19-PS for comparison purposes. Results of 19-PE+PP and 19-PS were prorated at a ratio of 9:1 to predict products that would result from independent conversion of the three polymers (Theoretical 19-PE+PP+PS, Fig. 7).

The total oil and naphtha (C_5 - C_9) yields of 19-PE+PP+PS were similar to the expected theoretical yields based on independent conversion (Fig. 7). The results suggest that PS and polyolefins convert independently and can be co-processed at these conditions without the need for separating PS from polyolefins before conversion. The compositions of naphtha and middle distillate fractions for each experiment are shown in Fig. 8(a) and Fig. 8(b), respectively. Co-processed PS and polyolefins produced naphtha and middle distillate fractions with higher aromatic contents than only polyolefins (Fig. 8). Both oil fractions have compositions that are similar to gasoline and diesel fuels, more so than oils from polyolefins alone, showing the benefit of increased aromatic contents in oils produced from co-processed PS and polyolefins.

7. Preliminary estimates of normalized energy recovery and environmental impacts for LP-HTP of PS compared to other treatment methods

This study was limited to lab-scale batch experiments. Future studies and optimization of LP-HTP methods in a continuous mode at pilot-plant scales are needed. To support future optimization and upscaling, preliminary analysis of energy recovery and environmental impacts from LP-HTP was conducted. The results were compared with those of other methods, specifically pyrolysis, SWL, incineration, and landfilling. Details of the analysis can be found in the Supplementary Materials (Fig. S8).

The energy recovery for each method (Fig. S8(a)) was calculated based on the difference between energy outputs [27,34,50] and required energy inputs [9,38,51–52]. Because of 99 % oil yields (Table 1) and low energy input requirements, LP-HTP was estimated to have the highest energy recovery compared to the other methods [27,34,50–52]. LP-HTP may have 7 %, 17 %, and up to 470 % higher energy recovery than pyrolysis, SWL, and incineration, respectively, while landfilling has no energy recovery.

Preliminary estimates for environmental impacts of LP-HTP methods were also compared with those of the other methods (Fig. S8(b)). The specific impacts compared were global warming potential (GWP), photochemical ozone creation potential (POCP), ozone layer depletion potential (OLDP), eutrophication potential (EP), acidification potential (AP), and abiotic depletion potential (ADP) [17,53–54]. LP-HTP methods were estimated to have lower GWP, POCP, EP, and AP impacts than pyrolysis because of less char sent to landfills (Table 1) [55–56]. Lower energy inputs for LP-HTP methods than SWL result in 3–4.8 times lower environmental impacts in all categories [9,38,51–52].

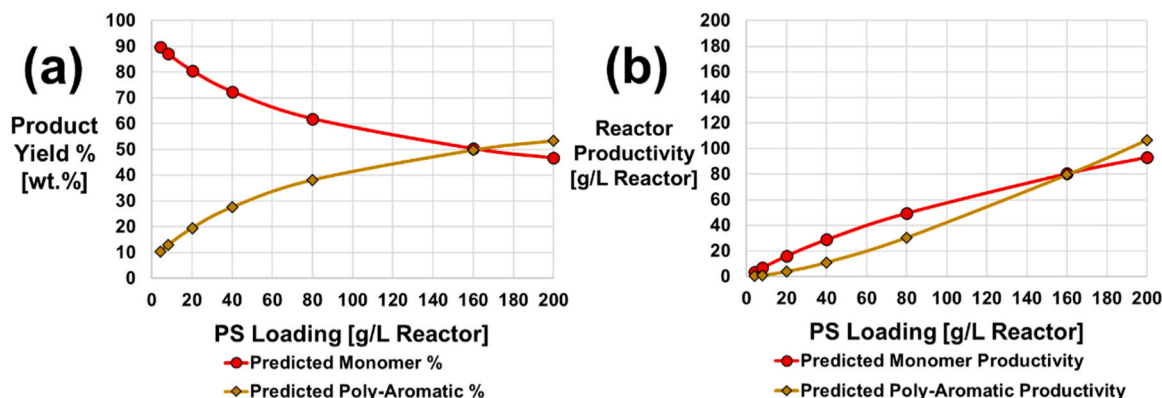


Fig. 6. Simulated (a) yield percentages [wt%] and (b) productivities [g/L Reactor] of monomers and poly-aromatics at various PS loadings.

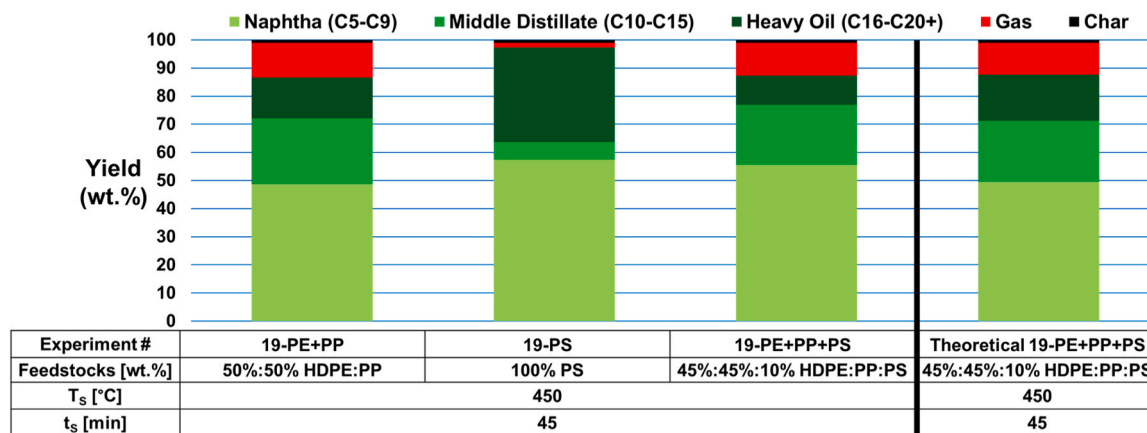


Fig. 7. Yields of naphtha, middle distillate, heavy oil, gas, and char from experiments studying the conversion of co-processed PS and polyolefins by LP-HTP methods.

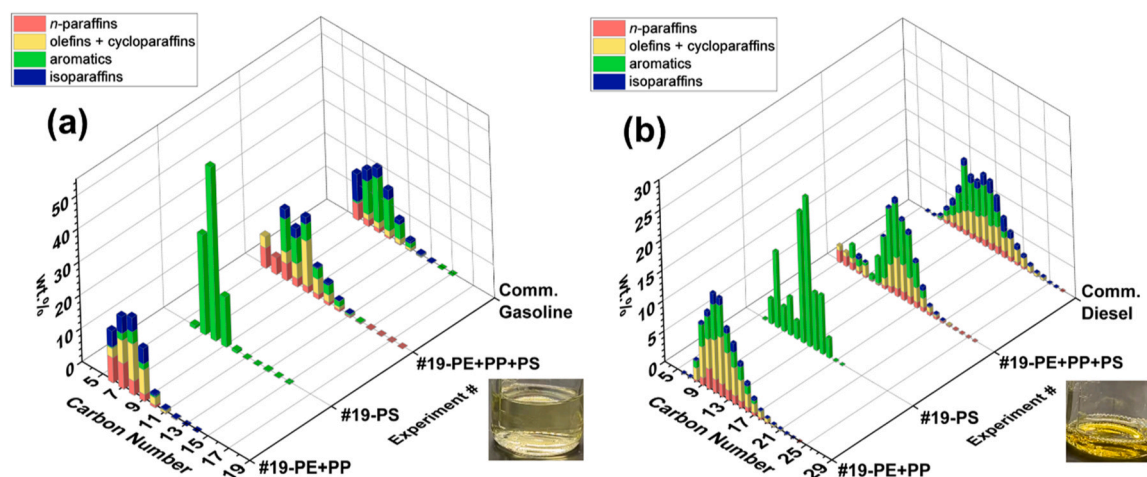


Fig. 8. Compositions of (a) naphtha and (b) middle distillate fractions from three experiments (19-PS, 19-PE+PP, and 19-PE+PP+PS) compared with those of commercial gasoline and diesel, respectively (y-axis). Weight percentages (z-axis) of four hydrocarbon classes (different colors) were plotted over a carbon number range (x-axis) of C₆–C₂₇. Images of the naphtha and middle distillate fractions from 19-PE+PP+PS are shown.

LP-HTP has lower impacts than incineration in all categories, including 30.2 times lower global warming potential and 11.3 times lower photochemical ozone creation potential [17,53,57]. LP-HTP notably has 40.5 times lower eutrophication potential than landfilling. The method has lower impacts than landfilling in all categories, except ozone layer depletion potential and abiotic depletion potential because of higher energy inputs [17,53,57–58]. The environmental detriments of landfilling also outweigh any perceived advantage over LP-HTP. Microplastics and char accumulated in landfills can cause future health impacts not included in this preliminary analysis [3,5,13]. LP-HTP can achieve high energy recovery by producing valuable oils while reducing the PS waste accumulation and associated environmental impacts.

8. Conclusions

Global polystyrene (PS) waste production reached 28 million tons annually, while PS recycling rates stay at 1.3 %. Conventional PS waste treatment methods of mechanical recycling and incineration have not reduced PS waste accumulation. Batch lab-scale low-pressure hydrothermal processing (LP-HTP) methods were developed for PS conversion to valuable oils in this study. If upscaled for commercial production, LP-HTP can overcome the limitations of current PS waste treatment methods.

LP-HTP methods produced higher oil yields from PS than pyrolysis and did not require a catalyst. Water acted as a diluent, resulting in much lower char formation (1–2 %) than pyrolysis (2–34 %, Table 1). This decreased char formation can reduce operating issues caused by char accumulation. Low water loadings (5 wt% water) resulted in higher monomer and BTEX yields, as well as lower operating pressures and energy than SWL (64 wt% water).

LP-HTP methods achieved 96–99 % oil yields from PS with minimal gas and char formation over a wide range of average reaction temperatures (T_A of 341–424 °C) and reaction times (t_E of 19–75 minutes). With a PS loading of 80 g/L, 67 % monomers (C₆–C₉) were produced at 414 °C for 45 minutes. Replicate LP-HTP experiments showed agreements within 1 % for oil, gas, and char yields, and agreements within 6 % for monomer and poly-aromatic (C₁₀–C₂₀+) yields. Oxidative stability studies showed that these oils had no oxidized hydrocarbons after 12 months.

Monomer yields were found to be limited by reversible reactions between monomers and poly-aromatics. A two-step kinetic model for PS conversion accounting for these reversible reactions was developed to aid process optimization. Temperature histories of 14 batch experiments were used for kinetic parameter estimation, such that the estimated parameters were independent of reactor heating or cooling rates. Nine additional experiments were conducted using various reaction temperatures, times, and PS loadings to test the predictive nature of the kinetic

model. The results showed that predicted yields of monomers and polyaromatics in oils agreed with observed yields to within 6 %. The close agreements in product yields showed the predictive nature of the kinetic model, which can be used for future process optimization and scale-up.

Kinetic model predictions were similar when using either full temperature histories or average temperatures (T_A). This agreement indicates that this process can more easily be scaled up using average temperatures. The model predicted that in a well-mixed reactor, a PS loading of 4 g/L can achieve a high monomer yield of 90 %. However, because of the reversible reaction, a trade-off was predicted between monomer yield and productivity, which should be considered in future process development.

As of 2021, 28 million tons of PS waste and 252 million tons of polyolefin waste were produced globally every year, representing about 70 % of the total plastic waste. The co-processing of 10 % PS with 90 % polyolefins was tested in this study. The results indicated that PS and polyolefins convert independently during co-processing, resulting in high oil yields (87 %) and increased aromatic contents in oils compared to those from polyolefins alone. This result showed that PS and polyolefins can be co-processed without separating the polymers before conversion. Preliminary estimates indicated that LP-HTP methods can have up to 4.7 times higher energy recovery and lower environmental impacts than incineration. LP-HTP can convert PS waste to valuable oils, while reducing plastic waste accumulation in landfills and associated environmental impacts.

To realize the full potential of LP-HTP, efficient continuous processes aided by kinetic modeling, detailed techno-economic analysis, and life-cycle assessment are required in future studies. If PS wastes are collected and converted into valuable oils at commercial-scales, plastic waste accumulation rates and the associated environmental impacts can be reduced. These oils can be separated into pure monomers and used as feedstocks for new chemical products, supporting a circular use of hydrocarbons.

CRedit authorship contribution statement

Clayton Clarkson Gentilcore: Writing – review & editing, Writing – original draft, Visualization, Validation, Methodology, Investigation, Formal analysis, Data curation, Conceptualization. **Kai Jin:** Writing – review & editing, Writing – original draft, Visualization, Methodology, Investigation, Formal analysis, Data curation, Conceptualization. **Genesis Barzallo:** Writing – review & editing, Writing – original draft, Visualization, Validation, Methodology, Formal analysis, Data curation. **Petr Vozka:** Writing – review & editing, Writing – original draft, Visualization, Validation, Supervision, Methodology, Investigation, Funding acquisition, Formal analysis, Data curation. **Nien-Hwa Linda Wang:** Writing – review & editing, Writing – original draft, Visualization, Supervision, Resources, Project administration, Methodology, Investigation, Funding acquisition, Formal analysis, Conceptualization.

Declaration of Competing Interest

The authors declare that they have no known competing financial interests or personal relationships that could have appeared to influence the work reported in this paper.

Data availability

Data will be made available on request.

Acknowledgements

We thank Alec Milbourne of California State University, Los Angeles for his help with obtaining the GC-MS/FID data. This study was partially supported by the Norman and Jane Li Professorship Endowment and the Maxine Spencer Nichols Endowment of Davidson School of Chemical

Engineering at Purdue University. This study was partially supported by the National Science Foundation with Award HRD-2112554 and NSF PREM (DMR-1523588).

Clayton C. Gentilcore was supported by the Norman and Jane Li Endowment and Kai Jin was supported by the Maxine Spencer Nichols Endowment of the Davidson School of Chemical Engineering at Purdue University. Petr Vozka was partially supported by the National Science Foundation with Award HRD-2112554. Genesis Barzallo was supported by NSF PREM (DMR-1523588).

Appendix A. Supporting information

Supplementary data associated with this article can be found in the online version at doi:10.1016/j.jece.2024.113836.

References

- [1] L.K. Ncube, A.U. Ude, E.N. Ogunmuyiwa, R. Zulkifli, I.N. Beas, An overview of plastic waste generation and management in food packaging industries, *Recycling* 6 (1) (2021) 12.
- [2] United Nations Environment Programme (UNEP). (2022). *Visual feature: Beat plastic pollution*. (<https://www.unep.org/interactives/beat-plastic-pollution/>).
- [3] United Nations Environment Programme (2021). *From Pollution to Solution: A global assessment of marine litter and plastic pollution*. Nairobi.
- [4] R. Geyer, J.R. Jambeck, K.L. Law, Production, use, and fate of all plastics ever made, *Sci. Adv.* 3 (7) (2017) e1700782.
- [5] P. Landrigan, C. Symeonides, H. Raps, S. Dunlop, The global plastics treaty: why is it needed?, *Lancet* 402 (10419) (2023) 2274–2276.
- [6] X. Zhao, M. Korey, K. Li, K. Copenhaver, H. Tekinalp, S. Celik, S. Ozcan, Plastic waste upcycling toward a circular economy, *Chem. Eng. J.* 428 (2022) 131928.
- [7] W.T. Chen, K. Jin, N.H. Linda Wang, Use of supercritical water for the liquefaction of polypropylene into oil, *ACS Sustain. Chem. Eng.* 7 (4) (2019) 3749–3758.
- [8] K. Jin, P. Vozka, G. Kilaz, W.T. Chen, N.H.L. Wang, Conversion of polyethylene waste into clean fuels and waxes via hydrothermal processing (HTP), *Fuel* 273 (2020) 117726.
- [9] K. Jin, P. Vozka, C. Gentilcore, G. Kilaz, N.H.L. Wang, Low-pressure hydrothermal processing of mixed polyolefin wastes into clean fuels, *Fuel* 294 (2021) 120505.
- [10] N. Chaukura, W. Gwenzli, T. Bunhu, D.T. Ruziwa, I. Pumure, Potential uses and value-added products derived from waste polystyrene in developing countries: a review, *Resour., Conserv. Recycl.* 107 (2016) 157–165.
- [11] United States Environmental Protection Agency. (2020, December). *Advancing Sustainable Materials Management: 2018 Tables and Figures Assessing Trends in Materials Generation and Management in the United States*. (https://www.epa.gov/sites/default/files/2021-01/documents/2018_tables_and_figures_dec_2020_fnl_508.pdf).
- [12] Recycling Today. (2019, April 24). *Polystyrene recycling programs expand despite bans*. (<https://www.recyclingtoday.com/news/polystyrene-recycling-programs-expand-despite-bans/>).
- [13] D. Choi, J. Bang, T. Kim, Y. Oh, Y. Hwang, J. Hong, In vitro chemical and physical toxicities of polystyrene microfragments in human-derived cells, *J. Hazard. Mater.* 400 (2020) 123308.
- [14] O. Eriksson, G. Finnveden, Plastic waste as a fuel-CO 2-neutral or not, *Energy Environ. Sci.* 2 (9) (2009) 907–914.
- [15] Al-Salem, S.M. (2019). *Energy production from plastic solid waste (PSW)*. In *Plastics to energy* (pp. 45–64). William Andrew Publishing.
- [16] S. Kwon, J. Kang, B. Lee, S. Hong, Y. Jeon, M. Bak, S.K. Im, Nonviable carbon neutrality with plastic waste-to-energy, *Energy Environ. Sci.* 16 (7) (2023) 3074–3087.
- [17] A. Vlasopoulos, J. Malinauskaitė, A. Žabnieńska-Góra, H. Jouhara, Life cycle assessment of plastic waste and energy recovery, *Energy* 277 (2023) 127576.
- [18] The American Society of Mechanical Engineers (ASME). (2022, June 6). *Waste to energy as a replacement for landfills*. ASME. (<https://www.asme.org/topics-resources/content/engineers-make-the-case-for-waste-to-energy>).
- [19] Z.O. Schyns, M.P. Shaver, *Mechanical recycling of packaging plastics: a review*, *Macromol. rapid Commun.* 42 (3) (2021) 2000415.
- [20] K. Ragaert, L. Delva, K. Van Geem, Mechanical and chemical recycling of solid plastic waste, *Waste Manag.* 69 (2017) 24–58.
- [21] Chen, W.T.G. (2021). *Chemical Recycling of Mixed Plastics and Valuable Metals in the Electronic Waste Using Solvent-Based Processing* (No. DOE-UML-0007897). University of Massachusetts Lowell; The REMADE Institute of Sustainable Manufacturing Innovation Alliance Corp.
- [22] L. Anderson, E. Yu, W.T. Chen, Chemical recycling of mixed plastics in electronic waste using solvent-based processing, *Processes* 10 (1) (2021) 66.
- [23] I.M. Maafa, Pyrolysis of polystyrene waste: a review, *Polymers* 13 (2) (2021) 225.
- [24] Cavinaw, B., Crawford, S., Lamaze, S., Allen, D., Christenson, E., & Rumford, M. (2020). U.S. Patent No. 10,731,080. Washington, DC: U.S. Patent and Trademark Office.
- [25] Pyzyk, K. (2020, October 7). *Plastic processors moving ahead on polystyrene recycling plant in Illinois*. Waste Dive. (<https://www.wastedive.com/news/plastic-agilyx-polystyrene-chemical-recycling-illinois/586321/>).

- [26] Patel, D., Moon, D., Tangri, N., & Wilson, M. (2020, July 28). *All Talk and No Recycling: An Investigation of the U.S. "Chemical Recycling" Industry*. Global Alliance for Incinerator Alternatives (GAIA). (https://www.no-burn.org/wp-content/uploads/2021/11/All-Talk-and-No-Recycling_July-28-1.pdf).
- [27] D.S. Achilias, I. Kanelloupolou, P. Megalokonomos, E. Antonakou, A.A. Lappas, Chemical recycling of polystyrene by pyrolysis: potential use of the liquid product for the reproduction of polymer, *Macromol. Mater. Eng.* 292 (8) (2007) 923–934.
- [28] J. Nisar, G. Ali, A. Shah, M. Iqbal, R.A. Khan, F. Anwar, M.S. Akhter, Fuel production from waste polystyrene via pyrolysis: kinetics and products distribution, *Waste Manag.* 88 (2019) 236–247.
- [29] V. Kumar, A. Khan, M. Rabnawaz, Efficient depolymerization of polystyrene with table salt and oxidized copper, *ACS Sustain. Chem. Eng.* 10 (19) (2022) 6493–6502.
- [30] B. Joshi, H. Raghav, A. Agrawal, B.P. Vempatapu, A. Ray, B. Sarkar, Sustainable production of styrene from catalytic recycling of polystyrene over potassium promoted Fe–Al 2 O 3 catalyst, *Sustain. Energy Fuels* 7 (5) (2023) 1256–1264.
- [31] G. Albor, A. Mirkouei, A.G. McDonald, E. Struhs, F. Sotoudehnia, Fixed bed batch slow pyrolysis process for polystyrene waste recycling, *Processes* 11 (4) (2023) 1126.
- [32] D.K. Ojha, R. Vinu, Resource recovery via catalytic fast pyrolysis of polystyrene using zeolites, *J. Anal. Appl. Pyrolysis* 113 (2015) 349–359.
- [33] V. Daligaux, R. Richard, M.H. Manero, Deactivation and regeneration of zeolite catalysts used in pyrolysis of plastic wastes—a process and analytical review, *Catalysts* 11 (7) (2021) 770.
- [34] H. Kwak, H.Y. Shin, S.Y. Bae, H. Kumazawa, Characteristics and kinetics of degradation of polystyrene in supercritical water, *J. Appl. Polym. Sci.* 101 (1) (2006) 695–700.
- [35] B. Bai, H. Jin, C. Fan, C. Cao, W. Wei, W. Cao, Experimental investigation on liquefaction of plastic waste to oil in supercritical water, *Waste Manag.* 89 (2019) 247–253.
- [36] H. Ke, T. Li-Hua, Z. Zi-Bin, Z. Cheng-fang, Reaction mechanism of styrene monomer recovery from waste polystyrene by supercritical solvents, *Polym. Degrad. Stab.* 89 (2) (2005) 312–316.
- [37] National Institute of Standards and Technology (NIST). (2018). NIST Chemistry WebBook, SRD 69. Thermophysical Properties of Fluid Systems. <https://webbook.nist.gov/chemistry/liquid/>.
- [38] C. Un, C. Gentilcore, K. Ault, H. Gieng, P. Vozka, N.H.L. Wang, Low-pressure hydrothermal processing of disposable face masks into oils, *Processes* 11 (10) (2023) 2819.
- [39] H. Nishizaki, K. Yoshida, J.H. Wang, Comparative study of various methods for thermogravimetric analysis of polystyrene degradation, *J. Appl. Polym. Sci.* 25 (12) (1980) 2869–2877.
- [40] G.P. Ravanetti, M. Zini, A study on the thermal degradation kinetics of syndiotactic polystyrene by thermogravimetric analysis, *Thermochim. Acta* 207 (1992) 53–64.
- [41] R.W.J. Westerhout, J. Waanders, J.A.M. Kuipers, W.P.M. van Swaaij, Kinetics of the low-temperature pyrolysis of polyethylene, polypropylene, and polystyrene modeling, experimental determination, and comparison with literature models and data, *Ind. Eng. Chem. Res.* 36 (6) (1997) 1955–1964.
- [42] The Engineering ToolBox. (2017). Hydrocarbons - Physical Data. Engineering ToolBox. https://www.engineeringtoolbox.com/hydrocarbon-boiling-melting-flash-autoignition-point-density-gravity-molweight-d_1966.html.
- [43] P. Vozka, G. Kilaz, How to obtain a detailed chemical composition for middle distillates via GC× GC-FID without the need of GC× GC-TOF/MS, *Fuel* 247 (2019) 368–377.
- [44] L. Šindelarová, E.N. Luu, P. Vozka, Comparison of gas and kerosene oils chemical composition before and after hydrotreating using comprehensive two-dimensional gas chromatography, *J. Chromatogr. Open* 2 (2022) 100068.
- [45] Zeng, W.R., Chow, W.K., & Yao, B. (2007). Chemical kinetics and mechanism of polystyrene thermal decomposition. In *Asia-Oceania Symp. Fire Sci. Technol. Fire Chem.*
- [46] A.M. Mebel, A. Landera, R.I. Kaiser, Formation mechanisms of naphthalene and indene: from the interstellar medium to combustion flames, *J. Phys. Chem. A* 121 (5) (2017) 901–926.
- [47] K.B. Park, Y.S. Jeong, B. Guzelciftci, J.S. Kim, Two-stage pyrolysis of polystyrene: pyrolysis oil as a source of fuels or benzene, toluene, ethylbenzene, and xylenes, *Appl. Energy* 259 (2020) 114240.
- [48] W.D. Lilac, S. Lee, Kinetics and mechanisms of styrene monomer recovery from waste polystyrene by supercritical water partial oxidation, *Adv. Environ. Res.* 6 (1) (2001) 9–16.
- [49] S. Sinha, A. Raj, Polycyclic aromatic hydrocarbon (PAH) formation from benzyl radicals: a reaction kinetics study, *Phys. Chem. Chem. Phys.* 18 (11) (2016) 8120–8131.
- [50] R. Miandad, A.S. Nizami, M. Rehan, M.A. Barakat, M.I. Khan, A. Mustafa, J. D. Murphy, Influence of temperature and reaction time on the conversion of polystyrene waste to pyrolysis liquid oil, *Waste Manag.* 58 (2016) 250–259.
- [51] A. Fivga, I. Dimitriou, Pyrolysis of plastic waste for production of heavy fuel substitute: a techno-economic assessment, *Energy* 149 (2018) 865–874.
- [52] C. Moliner, G. Pasquale, E. Arato, Municipal plastic waste recycling through pyrogasification, *Energies* 17 (5) (2024) 1206.
- [53] F. Petrakopoulou, D. Iribarren, J. Dufour, Life-cycle performance of natural gas power plants with pre-combustion CO₂ capture, *Greenh. Gases: Sci. Technol.* 5 (3) (2015) 268–276.
- [54] Cashman, S., Arden, S., Morelli, B., Gray, J., Bartram, D., & Falatko, D. (2021). Life Cycle and Cost Assessments of Nutrient Removal Technologies in Wastewater Treatment Plants. Technical Report, EPA, Eastern Research Group. <https://www.epa.gov/system/files/documents/2023-06/life-cycle-nutrient-removal.pdf>.
- [55] R. Hermanns, A. Kraft, P. Hartmann, R. Meys, Comparative life cycle assessment of pyrolysis–recycling Germany’s sorted mixed plastic waste, *Chem. Ing. Tech.* 95 (8) (2023) 1259–1267.
- [56] G. Hu, H. Feng, P. He, J. Li, K. Hewage, R. Sadiq, Comparative life-cycle assessment of traditional and emerging oily sludge treatment approaches, *J. Clean. Prod.* 251 (2020) 119594.
- [57] The Engineering ToolBox. (2005). *Fuel gases - heating values*. Engineering ToolBox.
- [58] Y. Zhang, J. Liang, G. Zeng, W. Tang, Y. Lu, Y. Luo, W. Huang, How climate change and eutrophication interact with microplastic pollution and sediment resuspension in shallow lakes: a review, *Sci. Total Environ.* 705 (2020) 135979.

Glossary

T_S : set temperature (°C)
 t_S : set time (minutes)
 T_A : effective average reaction temperature (°C)
 t_E : effective reaction time (minutes)
Monomers: one-ring aromatic hydrocarbons in the carbon number range of C₆–C₉
Poly-Aromatics: multi-ring aromatic hydrocarbons in the carbon number range of C₁₀–C₂₀₊
Dimer: two-ring aromatic hydrocarbons in the carbon number range of C₁₀–C₁₇
Trimer: three-ring aromatic hydrocarbons in the carbon number range of C₁₆–C₁₉
Heavy Aromatic: aromatic hydrocarbons with three or more aromatic rings in the carbon number range of C₁₆–C₂₀₊
Naphtha: hydrocarbons (*n*-paraffins, isoparaffins, olefins, cycloparaffins, aromatics) in the carbon number range of C₅–C₉
Middle Distillate: hydrocarbons in the carbon number range of C₁₀–C₁₅
Heavy Oil: hydrocarbons in the carbon number range of C₁₆–C₂₀₊
MATLAB: Programming platform used for estimating best-fitting intrinsic kinetic parameters
ODE45: Ordinary Differential Equation Solver function
LSQNONLIN: Non-Linear Least-Squares Fitting function
Global Warming Potential (GWP): emissions of CO₂ equivalent (CO₂ eq.)
Photochemical Ozone Creation Potential (POCP): emissions of ethylene equivalent (C₂H₄ eq.)
Ozone Layer Depletion Potential (OLDP): emissions of trichlorofluoromethane equivalent (CFC-11 eq.)
Eutrophication Potential (EP): emissions of phosphate equivalent (PO₄³⁻ eq.)
Acidification Potential (AP): emissions of sulfur dioxide equivalent (SO₂ eq.)
Abiotic Depletion Potential (ADP): emissions of antimony equivalent (Sb eq.)

Variables

k_1 and k_2 , [min⁻¹]: Kinetic Rate Constant of First-Order Decomposition Reactions
 $k_{0,1}$ and $k_{0,2}$, [min⁻¹]: Pre-Exponential Factor of First-Order Decomposition Reactions
 k_B , [L•mol⁻¹•min⁻¹]: Kinetic Rate Constant of Second-Order Recombination Reactions
 $k_{0,B}$, [L•mol⁻¹•min⁻¹]: Pre-Exponential Factor of Second-Order Recombination Reactions
 $E_{a,x}$, [kJ•mol⁻¹]: Activation Energy of Reaction *x*
 R , [kJ•K⁻¹•mol⁻¹]: Molar Constant, R 8.3145×10⁻³ kJ•K⁻¹•mol⁻¹
 t_i , [min]: Initial Time
 t_f , [min]: Final Time
 T_{fb} , [K]: Average Temperature between Initial Time (t_i) and Final Time (t_f)
 $C_{j,b}$, [mol•L⁻¹]: Initial Concentration of Lumped Species *j*, such as Polystyrene (PS), Poly-Aromatics (PolyAro) or Monomers (Mono)
 $C_{j,f}$, [mol•L⁻¹]: Final Concentration of Lumped Species *j*